BRET Nano Q-body: A Nanobody-Based Ratiometric Bioluminescent Immunosensor for Point-of-Care Testing

Yinghui Yang[1], Akihito Inoue[1], Takanobu Yasuda[2], Hiroshi Ueda[2,†], Bo Zhu[2], Tetsuya Kitaguchi[2,*]

[1] Graduate School of Life Science and Technology, Tokyo Institute of Technology, Kanagawa, Japan

[2] Laboratory for Chemistry and Life Science, Institute of Innovative Research, Tokyo Institute of Technology, Kanagawa, Japan

[†] Deceased

[*] Correspondence:

Tetsuya Kitaguchi, Ph. D.

kitaguc.t.aa@m.titech.ac.jp

Keywords: *immunosensor, BRET, Quenchbody, nanobody, point-of-care testing*

Abstract

We developed a nanobody-based homogeneous bioluminescent immunosensor whose emission color changes by the bioluminescence resonance energy transfer (BRET) upon antigen addition to realize the one-pot analysis for point-of-care testing (POCT) and named it BRET nano Q-body. The NanoLuc luciferase and a cysteine-containing tag were fused to the N-terminal of the nanobody, which was subsequently labeled with fluorescent dye through a thiol-maleimide reaction. The nanobody employed in this proof-of-principle experiment recognizes methotrexate (MTX), a chemotherapy agent for cancer treatment. The BRET nano Q-body after fluorescent dye and linker optimization exhibited a more than 8-fold increase in emission ratio (TAMRA/Nluc) in a dose-dependent manner. We also found that its superior thermostability, endurance in organic solvents, reducing agents and detergents due to the robust structure of nanobody, as well as accommodation in biological fluids such as milk, serum, and whole blood without dilution, with limits of detection of 0.5, 1.6, and 3.7 nM, respectively. Furthermore, we performed lyophilization on BRET nano Q-body and made it into the paper device, greatly improving portability and allowing more than one month of storage in 25 ℃. The paper device also functioned properly in the aforementioned biological fluids without dilution and can be applied to therapeutic drug monitoring of MTX on site. We provided a powerful tool, BRET nano Q-body for POCT, and demonstrated its applicability in several biological fluids and the feasibility of paper devices, which is greatly expected as the pioneer for *in situ* detection in therapeutic, diagnostic, and environmental applications.

Introduction

Immunoassay is the analytical method utilizing antibody-antigen reaction to achieve specific and sensitive detection of substances, which possesses a wide range of applications in clinical diagnosis[1–3], food safety monitoring[4–6], and environmental assessment[7–9]. Various immunosensors are utilized in immunoassays, for example, homogeneous fluorescent dye-labeled immunosensors, termed "Quenchbodies" (Q-bodies)[10] employing various recombinant antibody fragments such as single-chain variable fragment (scFv)[8,11], fragment antigen-binding region (Fab)[12,13], and the variable region of heavy-chain antibodies (VHH, or nanobody)[14,15] have been fabricated, and served for the detection including small molecules, peptides, and proteins. The working principle of this fluorescent homogenous immunosensor is that the labeled fluorescent dye is quenched by the intrinsic tryptophan residues of antibodies through photoinduced electron transfer (PET) reactions and recovers its fluorescence by release of the dye upon antigen binding. Since their signal changes can be detected by simply mixing the analytes, it is considered one of the ideal tools for point-of-care testing (POCT). However, fluorescent homogeneous immunosensors including the Q-body generally suffer from the detection in biological fluids such as whole blood and milk, due to light scattering and autofluorescence, and the requirement of an external light source for excitation.

Several bioluminescent homogeneous immunosensors categorized under two working principles[16], complementation of split luciferase fragments[17] and bioluminescence resonance energy transfer (BRET)[18,19], have been developed to overcome these shortcomings of fluorescent homogeneous immunosensors. In principle, the bioluminescent immunosensors based on complementation are always two-fragment immunosensors, requiring separate preparation of the two fragments and is not easy to handle, whereas immunosensors based on BRET can be a single fragment and are user-friendly. Exploiting the advantage, we have also developed the BRET immunosensor, BRET Q-body[18], converting the fluorescence response of Q-body into BRET response by fusing NanoLuc to the N-terminal of scFv, which showed an enhanced response. Another BRET immunosensor, a luciferase-based indicator of drugs (LUCIDs)[19], which combines the fusion of antibody fragments to NanoLuc and SNAP-tag labeling with a fluorescent competitor of the antigen, was reported. These BRET immunosensors overcome the shortcomings of fluorescent immunosensors by being used without an external light source.

Although the emergence of BRET immunosensors has brought great convenience to POCT, the quantification of analytes in biological fluids without dilution such as milk and whole blood remained unknown. Detection in biological fluids including serum albumin, hemoglobin, and casein micelle requires a larger response of immunosensors, because impurities binding to or degrading immunosensors, or scattering of emission lead to low or even undetectable signal-to-background ratio[20]. Moreover, the performance of immunosensors tends to deteriorate in the further development for POCT such as lyophilization and paper devices, where the stability of immunosensors is expected. The variable region of heavy-chain antibody, nanobody from camelids not comprising light chain is known to be small and stable[21]. The hydrophobic interfaces between heavy and light chains in scFv are considered to be related to the antigen binding, which is lost at high temperatures due to VH-VL disassembly[22]. However, there is one domain in nanobody and this unique structure contributes to the stability of nanobody even in harsh environments, including the superior thermostability and excellent tolerance to organic solvents[23]. With these advantages, we assumed that nanobody was the hopeful candidate to fabricate a more robust bioluminescent immunosensor, BRET nano Q-body.

In our molecular design, NanoLuc, a cysteine-containing tag (Cys-tag)[24], and nanobody against MTX were arranged in the listed order. The working principle of BRET nano Q-body is that the binding of MTX releases the quenched TAMRA from MTX-VHH, which facilitates the access of TAMRA to NanoLuc and leads to the increase of BRET efficiency (Figure 1a). The linker between NanoLuc and Cys-tag was optimized to enhance the change in emission ratio (TAMRA/NanoLuc), allowing detection in biological fluid containing various impurities and scatters requiring a large response. Harnessing the enhanced durability afforded by nanobodies even in challenging environments, the evolution of paper-based devices is pushing the boundaries of practical applications by BRET nano Q-body. With its remarkable simplicity and sensitivity, this nanobody-based bioluminescent homogeneous immunosensor is poised to become a pivotal tool for POCT across diverse scenarios.

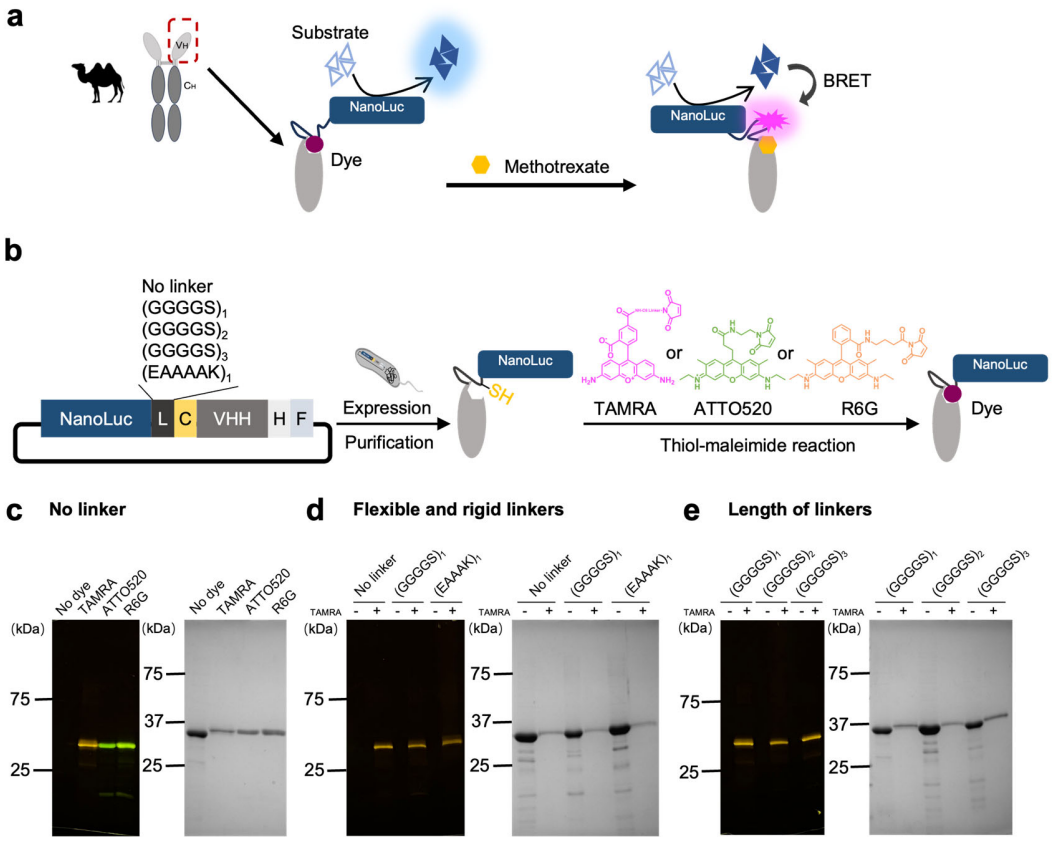

Figure 1. Fabrication of BRET nano Q-body. (a) The design and working principle of BRET nano Q-body. (b) The fabrication process of BRET nano Q-body containing various linkers (L: linker; C: cys-tag; H: 6×His tag; F: FLAG tag); (c) The SDS-PAGE of BRET nano Q-bodies with different dyes. (d) The SDS-PAGE of BRET nano Q-bodies with flexible $(GGGGS)_1$ and rigid $(EAAAK)_1$ linker. (e) The SDS-PAGE of BRET nano Q-bodies with different lengths of linkers.

Preparation of the BRET Nano Q-body

In the design of the BRET nano Q-body, NanoLuc is the energy donor, and the fluorescent dye is the energy acceptor. To realize the energy transfer, NanoLuc and a cysteine-containing tag (Cys-tag) for labeling fluorescent dye were fused to the N-terminus of MTX-VHH, which is a fragment from camelid antibody specifically bound to methotrexate (MTX), known as a drug for cancer treatment. Since the MTX-VHH was shown to function as a Q-body by fluorescence labeling[14], we employed it as a model antibody for the proof-of-principle experiment. The fluorescent dye was labeled to the cysteine residue through a thiol-maleimide reaction. Following our design, fluorescent dyes, linker flexibility and length were varied to reach higher response upon antigen binding (Figure 1b), and their further characterizations were performed later. To confirm the purification and dye labeling of candidate proteins for BRET nano Q-bodies, we performed the SDS-PAGE analysis. All main fluorescent and CBB-stained bands were consistent with the theoretical molecular mass of NanoLuc-MTXVHH (Figure 1c-e) and labeled fluorescence was identical to the expected color, thus we considered they were ready for further optical characterization.

Optimization of Linkers for BRET Nano Q-body

In the previous study, the response of nano Q-body by de-quenching was largest when TAMRA was labeled compared with ATTO520- or R6G-labeled ones. Nevertheless, we decided to examine the responses by labeling with these dyes, considering the possibility that the response was enhanced by additional changes in BRET efficiency upon antigen binding. When we measured the emission spectra of NanoLuc-TAMRA-MTXVHH, the emission intensity decreased at wavelengths around 450 nm, and increased around 580 nm after mixing with 1.0 μM MTX (Figure 2a). The increase in emission intensity around 580 nm was larger than the decrease around 450 nm. We considered that the decrease in emission intensity around 450 nm was caused by the release of TAMRA from MTXVHH upon MTX binding, which shortened the distance between NanoLuc and TAMRA, and increased BRET efficiency from NanoLuc to TAMRA, leading to a decrease in the emission of NanoLuc. We considered that the larger increase around 580 nm was attributed to the change in BRET efficiency and an additional response derived from the de-quenching of TAMRA as well as nano Q-body. When MTX was added to NanoLuc-MTXVHH labeled with ATTO520 and R6G, we found little decrease around 450 nm, but a small increase around 550 and 570 nm, respectively (Figure 2b-c). These can be

interpreted as little change in BRET efficiency and a small de-quenching of dyes upon the addition of MTX, which is consistent with the response from nano Q-body labeled with ATTO520 or R6G. Since the change in BRET ratio (fluorescent dye/NanoLuc) of NanoLuc-MTXVHH labeled with TAMRA, ATTO520, and R6G were 5.4, 1.3, and 1.1-fold, respectively, we chose TAMRA-labeled prototype for further optimization.

To improve the response calculated by the emission ratio of NanoLuc-TAMRA-MTXVHH, we optimized the flexibility and length of linkers between NanoLuc and TAMRA, which is reasonable because BRET efficiency is usually related to the orientation and distance between donor and acceptor. When flexible linker $(GGGGS)_1$ or rigid linker $(EAAAK)_1$ was introduced, the response was largest with flexible linker (Figure 2d). Next, when the length of the flexible linker was changed from $(GGGGS)_1$ to $(GGGGS)_2$ or $(GGGGS)_3$, the response was largest with $(GGGGS)_1$ linker (Figure 2e). Optimization of the linker led to an increase in the BRET efficiency, which is a larger decrease in emission around 450 nm, upon adding antigen (Figure 2f). We also examine the response solely caused by the de-quench of TAMRA after the addition of antigen by applying a 535 nm excitation light, and found the responses of 3.5-, 5.7-, and 5.4-fold for no linker, flexible linker, and rigid linker variants, respectively (Figure S2). This difference may reflect that the insertion of the linker between NanoLuc and TAMRA allowed the release of TAMRA from MTXVHH, which had been inhibited by the steric hindrance from NanoLuc. Taken together, these results suggest that optimization of the linker increased the change in both BRET efficiency and de-quenching for the development of BRET nano Q-body.

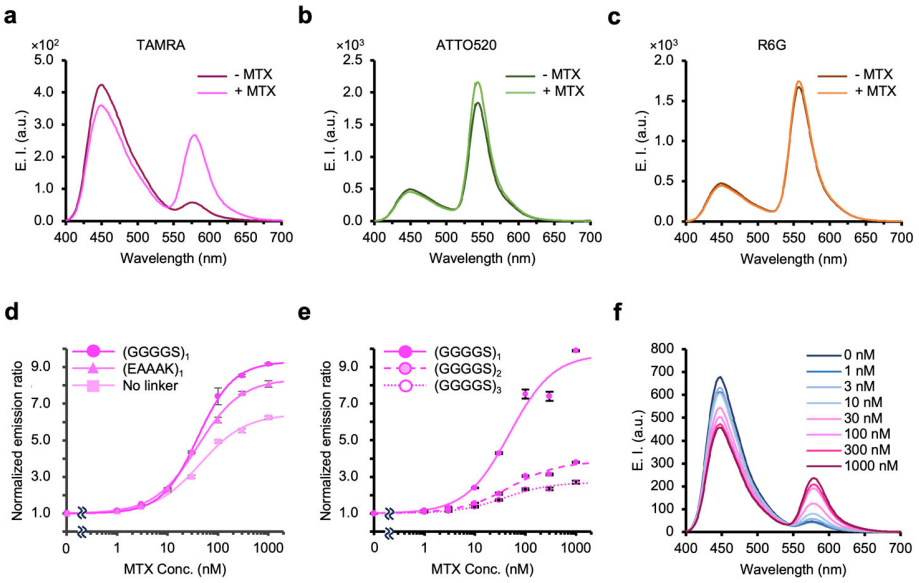

Figure 2. The characterization of BRET nano Q-bodies. (a) The emission spectra of NanoLuc-TAMRA-MTXVHH with or without 1.0 μM MTX. (b) NanoLuc-ATTO520-MTXVHH. (c) NanoLuc-R6G-MTXVHH. E.I.; emission intensity. (d) The dose-response relationship of NanoLuc-GGGGS$_1$-TAMRA-MTXVHH (circle), NanoLuc-EAAAK$_1$-TAMRA-MTXVHH (triangle) and NanoLuc-TAMRA-MTXVHH (square). Data are shown as the mean ± SD (n = 3). (e) The dose-response relationship using the emission ratio of NanoLuc-GGGGS$_1$-TAMRA-MTXVHH (closed circle), NanoLuc-GGGGS$_2$-TAMRA-MTXVHH (half-closed circle) and NanoLuc-GGGGS$_1$-TAMRA-MTXVHH (open circle). Data are shown as the mean ± SD (n = 3). (f) The emission spectra of NanoLuc-GGGGS$_1$-TAMRA-MTXVHH at various concentrations of MTX.

Stability Analysis of BRET Nano Q-body

Thermostability is one of the hallmarks of nanobody[25] in comparison with conventional antibody fragments. To test whether BRET nano Q-body is also thermostable, we examined its performance after 5 minutes of incubation at various temperatures with BRET Q-body as a comparison (Figure 3a). In case of change of the deterioration in EC_{50} of BRET nano Q-bodies, we applied 300 nM MTX and 100 nM BGP-C7[18] for the following measurements, which are ten times of EC_{50}. BRET nano Q-body remained more than 60% response after 37°C, 50°C 60°C, 70°C, 80°C or 95°C incubation, while there was less than 20% response left for BRET Q-body, which is derived from scFv against 7-aa peptide derived from bone Gla protein, after 50°C or higher incubation. Since portability is a great concern for point-of-care testing (POCT), we tested the performance of BRET nano Q-body and BRET Q-body after freeze-drying with or without lyoprotectant and stored as a powder rather than liquid. After adding water to dissolve the freeze-drying powders, BRET nano Q-body regained more than 90% response regardless of lyoprotectant, whereas there was around 30% response left without lyoprotectant, and around 60% response with 2.5% (w/v) or 5% (w/v) sucrose for BRET Q-body (Figure 3b).

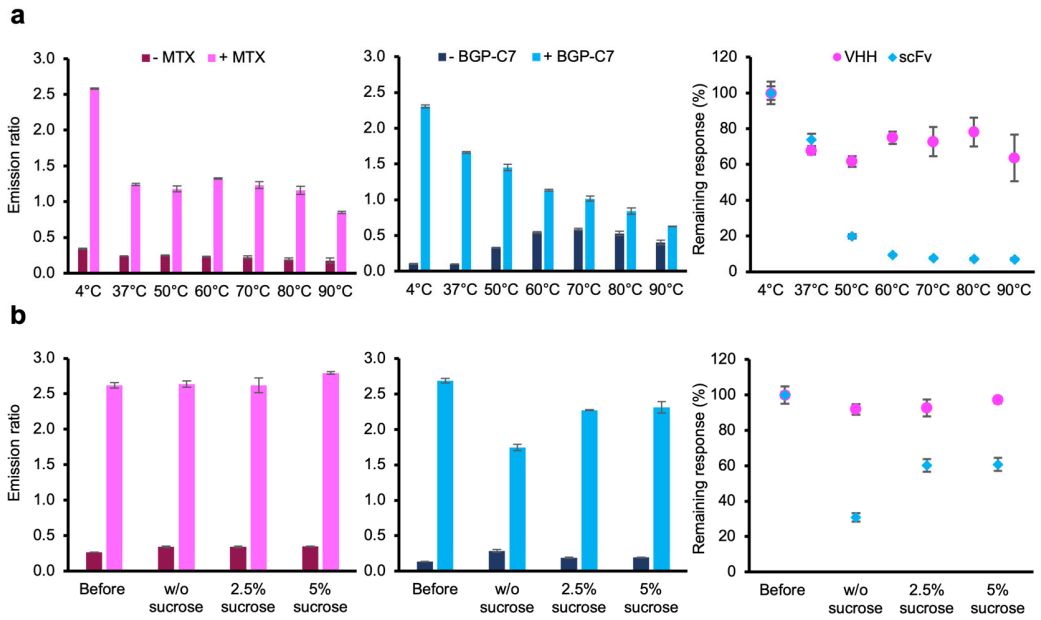

Figure 3. The thermostability and lyophilization test of BRET nano Q-body and BRET Q-body. (a) The emission ratio of NanoLuc-GGGGS$_1$-TAMRA-MTXVHH (magenta bar graph) and NanoLuc-TAMRA-scFv-BGP (blue bar graph) with or without 300 nM MTX and 100 nM BGP-C7, respectively, after 5 minutes incubation at varied temperatures. The concentrations of antigens are 10 times of EC_{50}. The scatter graph shows the comparison of the remaining response between of BRET nano Q-body (magenta dot) and BRET Q-body (blue dot). (b) The emission ratio of NanoLuc-GGGGS$_1$-TAMRA-MTXVHH (magenta bar graph), NanoLuc-TAMRA-scFv-BGP (blue bar graph) after lyophilization. The scatter graph shows the comparison of the remaining responses. All data are shown as the mean ± SD (n = 3).

Nanobody is also known for the tolerance in organic solvents[23], which are frequently used to dissolve substrate and pretreat analytes, and the presence of these residual solvents may disturb the measurements. To investigate the tolerance of BRET nano Q-body against organic solvents, we performed the measurements in DMSO, methanol, ethanol, and acetonitrile, which are commonly utilized in analytical chemistry and biological research. BRET nano Q-body maintained more than 35% of maximum response in 30% (v/v) DMSO and methanol while BRET Q-body was less than 15% (v/v) (Figure 4a-b). Both BRET nano Q-body and BRET Q-body were less tolerable in ethanol and acetonitrile than DMSO and methanol (Figure 4c-d), whereas BRET nano Q-body consistently showed a higher response than BRET Q-body at the same concentrations of organic solvents

In addition to organic solvents, reducing agents and detergents are commonly used in the inactivation of virus and lysing lipid complexes in pretreatment. To evaluate their effects on BRET nano Q-body, we examined the performance of BRET nano Q-body in reducing agents, DTT and β-ME, and detergents, Tween 20 and Triton X-100. BRET nano Q-body showed a larger response, and there were more than 50% and 70% responses left in 0.4 M DTT and β-ME, respectively (Figure 5a-b). Surprisingly, BRET nano Q-body remained around 100% response at all concentrations of Tween 20 and Triton X-100, while there was around, or less than 20% response left in BRET Q-body when the concentration of detergents was higher than 0.5% (Figure 5c-d).

Based on these results, BRET nano Q-body exhibited superiority in harsh environments, such as high temperature, organic solvent, reducing agent, and detergent as well as after lyophilization due to the robust structure of nanobody. And the thermostability of NanoLuc was enhanced compared with other luciferases[26]. Therefore, BRET nano Q-body is expected to be a practical tool for POCT in a wide range of applications.

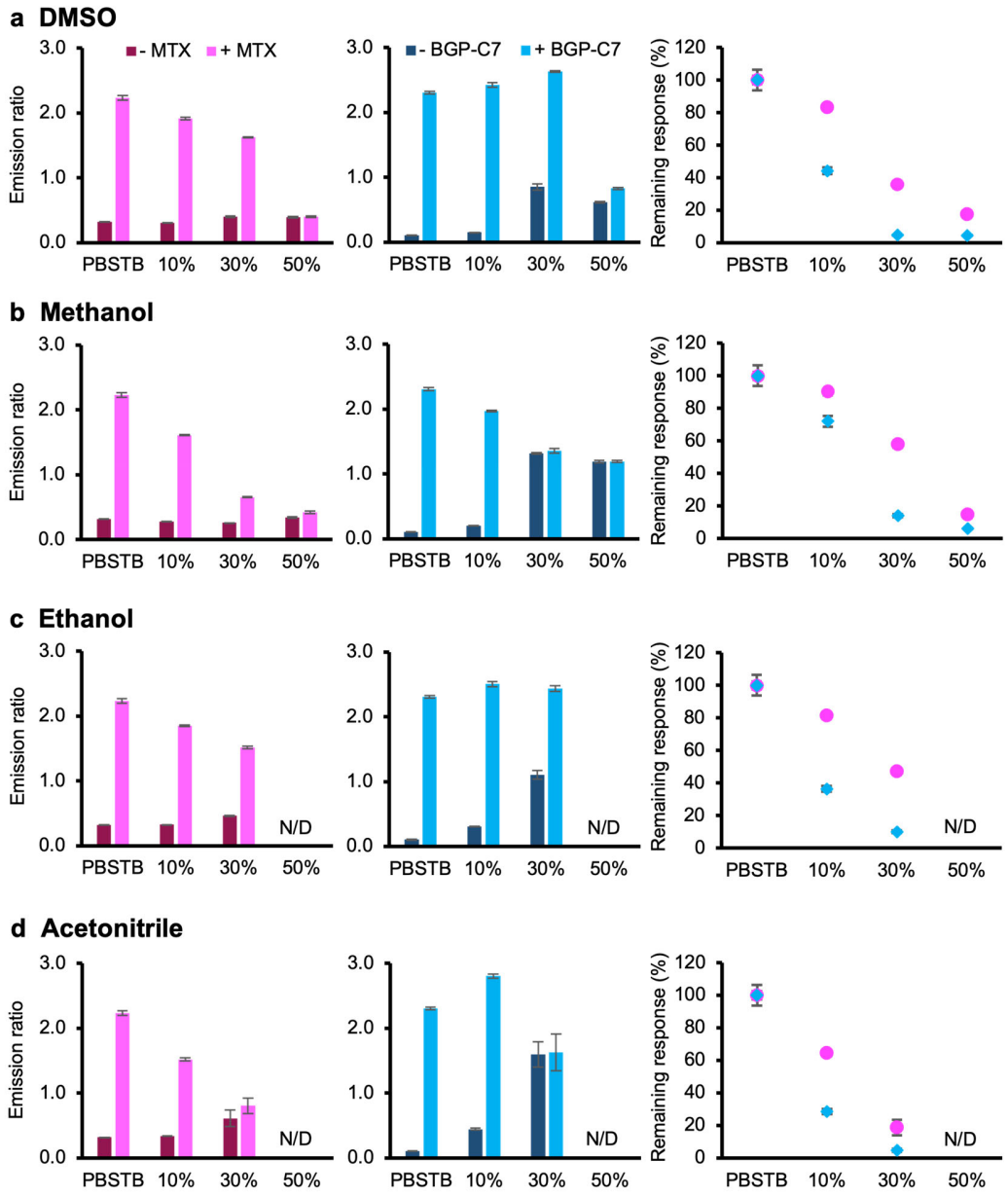

Figure 4. The tolerance in organic solvents of BRET nano Q-body and BRET Q-body. The emission ratio of NanoLuc-GGGGS$_1$-TAMRA-MTXVHH (magenta bar graph) and NanoLuc-TAMRA-scFv-BGP (blue bar graph) with or without 300 nM MTX and 100 nM BGP-C7, respectively, in various organic solvents. (a) dimethyl sulfoxide. (b) methanol. (c) ethanol. (d) acetonitrile. The scatter graph shows the comparison of the remaining response between of BRET nano Q-body (magenta dot) and BRET Q-body (blue dot). N/D, not detectable; the emission intensity was very small, and negative value after subtracting the background. All data are shown as the mean ± SD (n = 3).

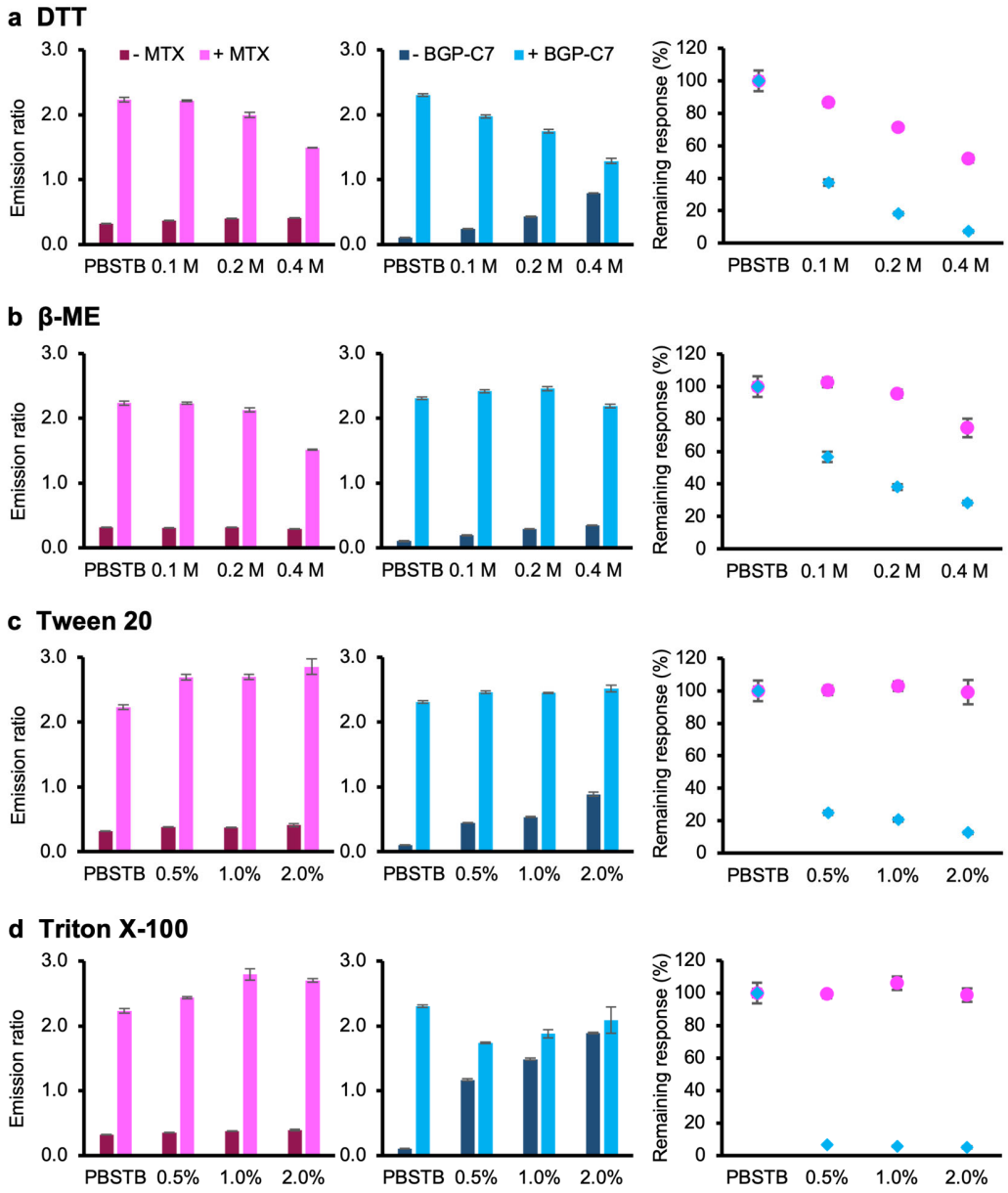

Figure 5. The tolerance against reducing agents and detergents of BRET nano Q-body and BRET Q-body. The emission ratio of NanoLuc-GGGGS$_1$-TAMRA-MTXVHH (magenta bar graph) and NanoLuc-TAMRA-scFv-BGP (blue bar graph) with or without 300 nM MTX and 100 nM BGP-C7, respectively, in various organic solvents. (a) dithiothreitol. (b) β-mercaptoethanol. (c) Tween 20. (d) Triton X-100. The scatter graph shows the comparison of remaining response between of BRET nano Q-body (magenta dot) and BRET Q-body (blue dot). All data are shown as the mean ± SD (n = 3).

Application of BRET Nano Q-body for Biological Fluids

Tools used in POCT are expected to function properly when working with biological fluids. To evaluate the efficacy of BRET nano Q-body, the performance of BRET nano Q-body was investigated in milk, serum, and whole blood by both fluorescence and bioluminescence. Although the fluorescent signal upon adding antigen became negative value after subtracting the background signal in milk, serum, and whole blood caused by high background, likely due to light scattering and autofluorescence (Figure 6a), they were successfully detected by bioluminescence in a dose-dependent manner (Figure 6b, c). Interestingly, the maximum responses in milk (8.7-fold), serum (9.2-fold), and whole blood (11.2-fold) were higher than in PBSTB (7.6-fold) (Figure 6c, Table 1). This is consistent with our previous results[27,28] that the crowding effects due to the complex components such as proteins and lipid from these matrices results in deeper quenching. Moreover, the values of the limit of detection (LOD) in PBSTB, milk, serum, and whole blood were 1.3, 0.5, 1.6, and 3.7 nM, respectively (Table 1), and these values meet the requirement of MTX monitoring during the chemotherapy on the cytotoxicity alert concentration (10-20 μM) and sufficient clearance (< 10 nM)[29]. To further improve the portability, we developed the paper device with BRET nano Q-body by freeze-drying and verified its function after storage at 25 ℃ (Figure 6d). When MTX was added to the paper device along with the substrate, the change of emission color was able to be recognized by a camera on a smartphone and even by the naked eye in a dark box (Figure S3). Although the maximum responses and LOD of the paper device were less than the liquid without freeze-drying, the sensitivity of BRET nano Q-body was maintained enough to be used for therapeutic drug monitoring in patient blood (Figure 6e, Table 1). Taken together, these results suggest that BRET nano Q-body is greatly expected to serve as a powerful tool for POCT.

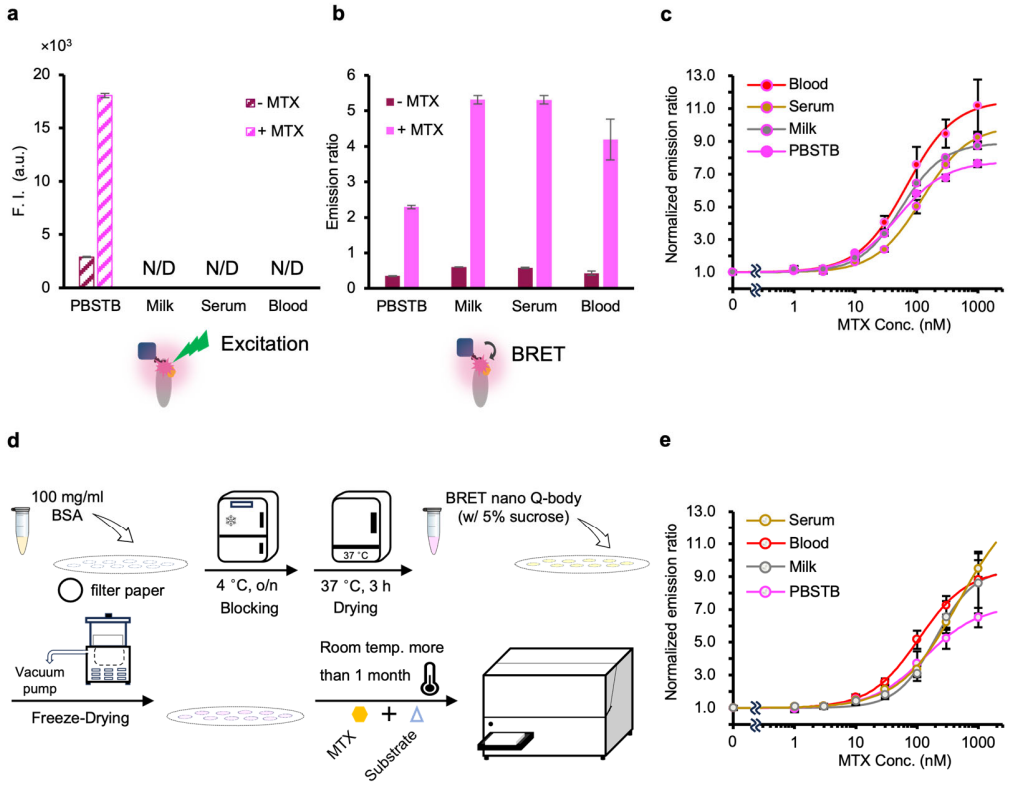

Figure 6. BRET nano Q-body response on paper device in biological fluids. (a) The fluorescence intensity of NanoLuc-GGGGS$_1$-TAMRA-MTXVHH with or without 300 nM MTX in various biological fluids. N/D, not detectable; the fluorescence intensity was negative value after subtracting the background, which is very high because of light scattering. F.I.; fluorescence intensity. (b) The emission ratio of NanoLuc-GGGGS$_1$-TAMRA-MTXVHH in various biological fluids. (c) The dose-response relationship using the emission ratio of NanoLuc-GGGGS$_1$-TAMRA-MTXVHH in solution. (d) Preparation process of the paper device. (e) The dose-response relationship using the emission ratio of NanoLuc-GGGGS$_1$-TAMRA-MTXVHH on paper device. All data are shown as the mean ± SD (n = 3).

Table 1. The summarization in response, EC_{50} and LOD of BRET nano Q-bodies.

	Fluid	Response	EC_{50} (nM)	LOD (nM)
Before lyophilization	PBSTB	7.6-fold	49.0	1.3
	Milk	8.7-fold	56.3	0.5
	Serum	9.2-fold	122.4	1.6
	Blood	11.2-fold	68.4	3.7
Paper device	PBSTB	6.5-fold	136.4	9.7
	Milk	8.6-fold	201.9	20.7
	Serum	9.5-fold	480.8	3.9
	Blood	8.8-fold	107.5	6.0

Conclusion

Herein, we reported a bioluminescent homogeneous immunosensor with a large response by integration of NanoLuc and nanobody showing excellent endurance in lyophilization and harsh environments such as high temperature, organic solvent, reducing agents, and detergents, as well as a wide range of application for biological fluids as a POCT tool. In the BRET nano Q-body, the ratiometric enhanced bioluminescence change allows the stable signal output even in complex matrices without dilution. The robustness of nanobody maintained the performance of paper devices meeting the requirement of the POCT for therapeutic drug monitoring. Furthermore, the employment of the nanobody offers wide target spectra in the future development of BRET nano Q-body. Therefore, we plan to expand the analyte from small molecules to proteins by taking advantage of the interchangeable feature of nanobodies, providing rapid and simple detection based on BRET nano Q-body. This bioluminescent immunosensor, which successfully functions even on a paper device will

revolutionize *in situ* detection, and be a new innovative tool in clinical diagnosis, food safety monitoring, and environmental assessment.

Materials and Methods

Materials

The *E. coli* strain XL10-Gold (Agilent, Santa Clara, CA, USA) was used for gene cloning. The *E. coli* strain SHuffle T7 Express *lysY* for protein production and restriction enzymes were purchased from New England Biolabs Japan (Tokyo, Japan). The gene fragments of NanoLuc were synthesized by Azenta (Massachusetts, USA). Oligonucleotides used in this study were synthesized by Integrated DNA Technologies and listed in Table S1. The KOD-Plus-Neo DNA polymerase and Ligation high ver. 2 were purchased from Toyobo (Osaka, Japan). In-Fusion HD Cloning Kit and TALON metal affinity resin were obtained from Clontech (Takara Bio, Shiga, Japan). MTX was purchased from Nacalai Tesque (Kyoto, Japan). C-terminal peptides from BGP (BGP-C7, NH2-RRFYGPV-COOH) and 3×DYKDDDDK (3×FLAG) peptide were synthesized by LifeTein (South Plainfield, NJ, USA). Human pooled serum was purchased from DS Pharma (Osaka, Japan). Sheep whole blood was purchased from Japan Lamb Group (Tokyo, Japan). Other chemicals and reagents, unless otherwise indicated, were purchased from Fujifilm-Wako. The ultra-pure water was purified with a Milli-Q water purification system (Millipore, Billerica, MA, USA).

Construction of Plasmids

Five kinds of plasmids for BRET nano Q-bodies with different linkers (No linker; $GGGGS_n$, n = 1 ~ 3; $EAAAK_1$) were constructed. pNL-SQ(KTM219)[18] and pSQ-MTXVHH[14] digested by restriction enzyme (AgeI-HF and BamHI-HF) were used to obtain the vector and insert of pBQ-Nluc-MTXVHH, respectively. Ligation was performed in subsequence with Ligation high Ver.2. Next, pBQ-Nluc-MTXVHH was digested by EagI-HF and XhoI to generate the vector for linker adjustment and used as the template to amplify $GGGGS_n$ (n = 1 ~ 3)-, $EAAAK_1$-MTXVHH fragments. Inf_Nluc_EagI_back and Overlap_G4S_NlucMTX_for were used to amplify the fragment NanoLuc-$GGGGS_1$. Overlap_G4S_NlucMTX_back and Inf_Nluc_XhoI_for were used to amplify fragment $GGGGS_1$-MTXVHH. NanoLuc-GGGGS-MTXVHH was generated by overlap PCR. NanoLuc-$GGGGS_2$-MTXVHH, NanoLuc-$GGGGS_3$-MTXVHH and NanoLuc-$EAAAK_1$-MTXVHH were generated with the same method. Finally, pBQ-Nluc-$GGGGS_n$-MTXVHH and pBQ-Nluc-$EAAAK_1$-MTXVHH were yielded through the In-Fusion HD Cloning Kit. The nucleotide sequences of primers were

244 listed in Supporting Information. All plasmids were purified with PureYield™ Plasmid Miniprep System
245 (Promega, WI, USA).
246 **Protein Production and Purification**
247 The *E. coli* strain SHuffle T7 Express *lysY* was used for protein production, which was cultured at 30 ℃ until
248 OD_{600} to 0.4 ~ 0.5, and induced in LB medium containing 0.4 mM isopropyl-β-D-thiogalactopyranoside at
249 16 ℃ for 18 hours. The pellet was collected by centrifuge (5000 g, 10 minutes) at 4 ℃ and resuspended with
250 phosphate buffer (1.15 g/L Na2HPO4, 5.75 g/L NaH2PO4, 17.53 g/L NaCl, pH 7.0). The *E. coli* was disrupted
251 with the Cell disruptor One Shot model (Constant System, UK) and centrifuged to collect the supernatant.
252 TALON Metal Affinity Resin was utilized to perform immobilized metal affinity chromatography for
253 purification. TALON Metal Affinity Resin was washed with binding buffer (phosphate buffer with 20 mM
254 imidazole, pH 7.4) and eluted with elution buffer (phosphate buffer with 500 mM imidazole, pH 7.4). A
255 MicroSpin G-25 Column was utilized to exchange the elution buffer of protein to PBS. The protein was
256 preserved in PBS buffer containing 15% glycerol at -30 ℃. The apparent molecular weight of the protein was
257 analyzed using sodium dodecyl sulfate-polyacrylamide gel electrophoresis (SDS-PAGE) (12.5%
258 polyacrylamide). The photo of SDS-PAGE gel after discoloration of the Coomassie Brilliant Blue staining was
259 taken by WSE-6100 LuminoGraph with ND-0.1 filter exposed for 1/3 s, and the concentration of proteins was
260 analyzed based on the BSA standard bands through the software CS Analyzer.
261 **Preparation of BRET Nano Q-body**
262 The purified proteins were labeled with fluorescent dyes through a thiol-maleimide reaction. 5 μM proteins
263 were treated with 2.5 mM Tris (2-carboxyethyl) phosphine hydrochloride (TCEP) for 1 hour at 25 ℃ in a dark
264 place to reduce the cystine residue. Subsequently, 4-Azidobenzoic acid with a final concentration of 10 mM
265 was used to react with the remaining TCEP for 10 minutes on ice. After treatment, 50 μM 5-TAMRA C6-
266 maleimide (AAT Bioquest, California, USA), ATTO520-maleimide, ATTO Rho6G (R6G)-maleimide (ATTO-
267 TEC GmbH, Siegen, German) were reacted with the proteins for 2 hours in a dark environment at 25 ℃.
268 BRET nano Q-body was mixed with Anti-FLAG M2 magnetic beads for purification. To remove the unlabeled
269 dye, the beads after binding overnight at 4 ℃ were washed with PBS (w/ 0.1% brij35) 12 times. The BRET
270 nano Q-body was eluted in 150 μg/ml 3 × FLAG peptide for 30 minutes. The concentration of BRET nano Q-

body was analyzed on SDS-PAGE as described above. The fluorescence of SDS-PAGE bands was observed with a 530LP filter under the 500 nm excitation light before Coomassie Brilliant Blue staining.

Bioluminescence and Fluorescence Measurement of BRET Nano Q-body

BRET nano Q-body was diluted in PBS containing 0.05% Tween 20 and 0.1% BSA (PBSTB) to the concentration of 15 nM. The bioluminescence and fluorescence spectra were measured in a quartz microcuvette (5 mm × 5 mm) utilizing an FP-8500 spectrofluorometer (Jasco, Tokyo, Japan). The bioluminescence measurement condition file is set to scan the wavelength from 400 nm to 700 nm with a scanning speed of 200 nm/min. In the bioluminescence measurement, the emission intensity of PBSTB was measured in advance. The BRET nano Q-bodies spiked with MTX (0 ~ 1000 nM) were mixed with Coelenterazine h (final concentration: 5 μg/ml) for 40 seconds reaction. In the fluorescence measurement, NanoLuc-MTXVHH labeled with TAMRA, ATTO520 and R6G was measured. The fluorescence measurement condition file is set to scan the wavelength from 560 nm to 700 nm with a scanning speed of 200 nm/min. The excitation wavelength is 547 nm with a bandwidth of 5 nm to measure NanoLuc-MTXVHH labeled with TAMRA.

The dose-response curves were drawn based on the bioluminescence measurement with a microplate-based spectrophotometer CLARIOStar (BMG Labtech Japan, Saitama, Japan) by measuring at the emission peak wavelength of NanoLuc and fluorescent dyes. After 20 minutes of incubation at 25 ℃, 1 nM BRET nano Q-body and BRET Q-body containing 0 ~ 1000 nM antigen were added in triplicate to a 96-well white half-well plate. The emission intensity was measured immediately after the addition of Coelenterazine h (final concentration: 5 μg/ml). For fluorescence measurement, a 96-well black half-well plate was utilized at the excitation wavelengths of 497 nm with a bandwidth of 14 nm, 535 nm with a bandwidth of 20 nm, and 540 nm with a bandwidth of 20 nm for ATTO520-, TAMRA-, and R6G-labeled BRET nano Q-body, respectively. Dose-response curves were fitted to a modified four-parameter logistic equation (equation 1), where the minimum asymptote (a) was fixed as 1 and c was estimated as EC_{50}, utilizing SciDAVis (https://scidavis.sourceforge.net/). The LOD was calculated as the concentration corresponding to the mean blank value plus 3 times the standard deviation (SD) for each assay.

$$y = d + \frac{a - d}{1 + \left(\frac{x}{c}\right)^{b}} \quad (1)$$

Preparation and Measurement with Paper Device

The qualitative filter paper was cut with a diameter of 5 mm and blocked with 100 mg/ml BSA overnight. After drying the filter paper, BRET nano Q-body containing 5% (v/v) sucrose was added to the dried paper followed by lyophilization. The prepared paper devices were stored in a dark place at 25 ℃. The paper-device-based measurement was performed with CLARIOStar. A piece of paper device was put at the bottom of the well, and 100 µl matrix (PBSTB, milk, serum, blood) spiked with varied concentrations of MTX for each well was added to a 96-well half-well plate and incubated for 20 minutes in the dark at 25 ℃ before the measurement.

Bioluminescence Observation

To observe and take photos of bioluminescence, 10 µl PBSTB spiked with MTX (0 ~1000 nM) was added to a piece of paper device and incubated for 20 minutes in the dark. Then 10 mg/ml Coelenterazine h (1/100 in v/v) was added to the paper device. The photos were taken with iPhone 13 (Apple, California, USA) at ISO8000, F1.6, exposed for 1.1 s in the dark box.

Data availability

Raw data are available from the corresponding author upon a reasonable request.

Author contributions

Y.Y. carried out, designed the experiments, and wrote the manuscript draft. T.K. and H.U. conceived the study. T.K., B.Z., and T.Y. designed experiments and edited the manuscript. A.I. supported designing experiments and analyzing data. All authors approved the final version of the manuscript.

Conflicts of interest

T.Y., H.U., B.Z. and T.K. received honoraria from HikariQ Health, Inc. for another unrelated project.

Acknowledgments

This work was supported by JSPS KAKENHI Grant Numbers JP22H05176 (T.K.), JP24K01264 (T.K.), JP21K14468 (B.Z.), and JP24H01123 (B.Z.) from the Japan Society for the Promotion of Science, Japan, and JST SPRING Grant Number JPMJSP2106 (Y.Y.) from the Japan Science and Technology Agency, Japan.

References

(1) Wang, M.; Shu, J.; Wang, Y.; Zhang, W.; Zheng, K.; Zhou, S.; Yang, D.; Cui, H. Ultrasensitive PD-L1-Expressing Exosome Immunosensors Based on a Chemiluminescent Nickel–Cobalt Hydroxide Nanoflower for Diagnosis and Classification of Lung Adenocarcinoma. *ACS Sens.* **2024**. https://doi.org/10.1021/acssensors.4c00954.

(2) Quintero-Campos, P.; Segovia-de los Santos, P.; Ibáñez-Echevarria, E.; Hernández-Fernández de Rojas, D.; Casino, P.; Lassabe, G.; González-Sapienza, G.; Maquieira, Á.; Morais, S. An Ultra-Sensitive Homologous Chemiluminescence Immunoassay to Tackle Penicillin Allergy. *Anal. Chim. Acta* **2022**, *1214*, 339940. https://doi.org/10.1016/j.aca.2022.339940.

(3) Eissa, S.; Zourob, M. Development of a Low-Cost Cotton-Tipped Electrochemical Immunosensor for the Detection of SARS-CoV-2. *Anal. Chem.* **2021**, *93* (3), 1826–1833. https://doi.org/10.1021/acs.analchem.0c04719.

(4) Xie, X.; Yang, X.; Zhang, Y.; Mao, F.; He, Z.; Sun, Z.; Zhang, S.; Liu, X. Ready-to-Use Ratiometric Bioluminescence Immunosensor for Detection of Ochratoxin a in Pepper. *Biosens. Bioelectron.* **2024**, *259*, 116401. https://doi.org/10.1016/j.bios.2024.116401.

(5) He, Y.; Wang, H.; Yu, Z.; Tang, X.; Zhou, M.; Guo, Y.; Xiong, B. A Disposable Immunosensor Array Using Cellulose Paper Assembled Chemiresistive Biosensor for Simultaneous Monitoring of Mycotoxins AFB1 and FB1. *Talanta* **2024**, *276*, 126145. https://doi.org/10.1016/j.talanta.2024.126145.

(6) Zhu, L.; Dong, X.-X.; Gao, C.-B.; Gai, Z.; He, Y.-X.; Qian, Z.-J.; Liu, Y.; Lei, H.-T.; Sun, Y.-M.; Xu, Z.-L. Development of a Highly Sensitive and Selective Electrochemical Immunosensor for Controlling of Rhodamine B Abuse in Food Samples. *Food Control* **2022**, *133*, 108662. https://doi.org/10.1016/j.foodcont.2021.108662.

(7) Zhang, Y.-Y.; Li, L.-H.; Wang, Y.; Wang, H.; Xu, Z.-L.; Tian, Y.-X.; Sun, Y.-M.; Yang, J.-Y.; Shen, Y.-D. Ultrasensitive and Rapid Colorimetric Detection of Paraquat via a High Specific VHH Nanobody. *Biosens. Bioelectron.* **2022**, *205*, 114089. https://doi.org/10.1016/j.bios.2022.114089.

(8) Zhang, L.; Dong, H.; Li, H.; Li, B.; Zhao, G.; Cai, H.; Chen, L.; Dong, J. Novel Signal-on Immunosensors for Rapid and Sensitive Detection of Microcystin-LR. *Microchem. J.* **2021**, *167*, 106295. https://doi.org/10.1016/j.microc.2021.106295.

(9) Messaoud, N. B.; dos Santos, M. B.; Vieira, A.; Garrido-Maestu, A.; Espiña, B.; Queirós, R. B. A Novel Portable Label-Free Electrochemical Immunosensor for Ultrasensitive Detection of Aeromonas Salmonicida in Aquaculture Seawater. *Anal. Bioanal. Chem.* **2022**, *414* (22), 6591–6600. https://doi.org/10.1007/s00216-022-04219-9.

(10) Abe, R.; Ohashi, H.; Iijima, I.; Ihara, M.; Takagi, H.; Hohsaka, T.; Ueda, H. "Quenchbodies": Quench-Based Antibody Probes That Show Antigen-Dependent Fluorescence. *J. Am. Chem. Soc.* **2011**, *133* (43), 17386–17394. https://doi.org/10.1021/ja205925j.

(11) Sasao, A.; Takaki, M.; Jeong, H.-J.; Yonemitsu, K.; Ohtsu, Y.; Tsutsumi, H.; Furukawa, S.; Morioka, H.; Ueda, H.; Nishitani, Y. Development of a Fluvoxamine Detection System Using a Quenchbody, a Novel Fluorescent Biosensor. *Drug Test. Anal.* **2019**, *11* (4), 601–609. https://doi.org/10.1002/dta.2520.

(12) Abe, R.; Jeong, H.-J.; Arakawa, D.; Dong, J.; Ohashi, H.; Kaigome, R.; Saiki, F.; Yamane, K.; Takagi, H.; Ueda, H. Ultra Q-Bodies: Quench-Based Antibody Probes That Utilize Dye-Dye Interactions with Enhanced Antigen-Dependent Fluorescence. *Sci. Rep.* **2015**, *4* (1), 4640. https://doi.org/10.1038/srep04640.

(13) Dai, Y.; Sato, Y.; Zhu, B.; Kitaguchi, T.; Kimura, H.; Ghadessy, F. J.; Ueda, H. Intra Q-Body: an Antibody-Based Fluorogenic Probe for Intracellular Proteins That Allows Live Cell Imaging and Sorting. *Chem. Sci.* **2022**, *13* (33), 9739–9748. https://doi.org/10.1039/D2SC02355E.

(14) Inoue, A.; Ohmuro-Matsuyama, Y.; Kitaguchi, T.; Ueda, H. Creation of a Nanobody-Based Fluorescent Immunosensor Mini Q-Body for Rapid Signal-On Detection of Small Hapten Methotrexate. *ACS Sens.* **2020**, *5* (11), 3457–3464. https://doi.org/10.1021/acssensors.0c01404.

(15) Inoue, A.; Yasuda, T.; Zhu, B.; Kitaguchi, T.; Murakami, A.; Ueda, H. Evaluation and Selection of Potent Fluorescent Immunosensors by Combining Fluorescent Peptide and Nanobodies Displayed on Yeast Surface. *Sci. Rep.* **2021**, *11* (1), 22590. https://doi.org/10.1038/s41598-021-02022-7.

(16) Qawee Rani, A.; Zhu, B.; Ueda, H.; Kitaguchi, T. Recent Progress in Homogeneous Immunosensors Based on Fluorescence or Bioluminescence Using Antibody Engineering. *Analyst* **2023**, *148* (7), 1422–1429. https://doi.org/10.1039/D2AN01913B.

(17) Ni, Y.; Rosier, B. J. H. M.; van Aalen, E. A.; Hanckmann, E. T. L.; Biewenga, L.; Pistikou, A.-M. M.; Timmermans, B.; Vu, C.; Roos, S.; Arts, R.; Li, W.; de Greef, T. F. A.; van Borren, M. M. G. J.; van Kuppeveld, F. J. M.; Bosch, B.-J.; Merkx, M. A Plug-and-Play Platform of Ratiometric Bioluminescent Sensors for Homogeneous Immunoassays. *Nat. Commun.* **2021**, *12* (1), 4586. https://doi.org/10.1038/s41467-021-24874-3.

(18) Takahashi, R.; Yasuda, T.; Ohmuro-Matsuyama, Y.; Ueda, H. BRET Q-Body: a Ratiometric Quench-Based Bioluminescent Immunosensor Made of Luciferase–Dye–Antibody Fusion with Enhanced Response. *Anal. Chem.* **2021**, *93* (21), 7571–7578. https://doi.org/10.1021/acs.analchem.0c05217.

(19) Xue, L.; Yu, Q.; Griss, R.; Schena, A.; Johnsson, K. Bioluminescent Antibodies for Point-of-Care Diagnostics. *Angew. Chem.* **2017**, *129* (25), 7218–7222. https://doi.org/10.1002/ange.201702403.

(20) Hall, M. P.; Kincaid, V. A.; Jost, E. A.; Smith, T. P.; Hurst, R.; Forsyth, S. K.; Fitzgerald, C.; Ressler, V. T.; Zimmermann, K.; Lazar, D.; Wood, M. G.; Wood, K. V.; Kirkland, T. A.; Encell, L. P.; Machleidt, T.; Dart, M. L. Toward a Point-of-Need Bioluminescence-Based Immunoassay Utilizing a Complete Shelf-Stable Reagent. *Anal. Chem.* **2021**, *93* (12), 5177–5184. https://doi.org/10.1021/acs.analchem.0c05074.

(21) Muyldermans, S. Nanobodies: Natural Single-Domain Antibodies. *Annu. Rev. Biochem.* **2013**, *82* (Volume 82, 2013), 775–797. https://doi.org/10.1146/annurev-biochem-063011-092449.

(22) Dumoulin, M.; Conrath, K.; Van Meirhaeghe, A.; Meersman, F.; Heremans, K.; Frenken, L. G. J.; Muyldermans, S.; Wyns, L.; Matagne, A. Single-Domain Antibody Fragments with High Conformational Stability. *Protein Sci.* **2002**, *11* (3), 500–515. https://doi.org/10.1110/ps.34602.

(23) He, T.; Wang, Y.; Li, P.; Zhang, Q.; Lei, J.; Zhang, Z.; Ding, X.; Zhou, H.; Zhang, W. Nanobody-Based Enzyme Immunoassay for Aflatoxin in Agro-Products with High Tolerance to Cosolvent Methanol. *Anal. Chem.* **2014**, *86* (17), 8873–8880. https://doi.org/10.1021/ac502390c.

(24) Jeong, H.-J.; Kawamura, T.; Dong, J.; Ueda, H. Q-Bodies from Recombinant Single-Chain Fv Fragment with Better Yield and Expanded Palette of Fluorophores. *ACS Sens.* **2016**, *1* (1), 88–94. https://doi.org/10.1021/acssensors.5b00089.

(25) Kunz, P.; Zinner, K.; Mücke, N.; Bartoschik, T.; Muyldermans, S.; Hoheisel, J. D. The Structural Basis of Nanobody Unfolding Reversibility and Thermoresistance. *Sci. Rep.* **2018**, *8* (1), 7934. https://doi.org/10.1038/s41598-018-26338-z.

(26) England, C. G.; Ehlerding, E. B.; Cai, W. NanoLuc: a Small Luciferase Is Brightening up the Field of Bioluminescence. *Bioconjug. Chem.* **2016**, *27* (5), 1175–1187. https://doi.org/10.1021/acs.bioconjchem.6b00112.

(27) Zhu, B.; Nosaka, N.; Kanamaru, S.; Dong, J.; Dai, Y.; Inoue, A.; Yang, Y.; Kobayashi, K.; Kitaguchi, T.; Iwasaki, H.; Koike, R.; Wakabayashi, K.; Ueda, H. Rapid and Sensitive SARS-CoV-2 Detection Using a Homogeneous Fluorescent Immunosensor Quenchbody with Crowding Agents. *Analyst* **2022**. https://doi.org/10.1039/D2AN01051H.

(28) Dong, J.; Miyake, C.; Yasuda, T.; Oyama, H.; Morita, I.; Tsukahara, T.; Takahashi, M.; Jeong, H.-J.; Kitaguchi, T.; Kobayashi, N.; Ueda, H. PM Q-Probe: a Fluorescent Binding Protein That Converts Many Antibodies to a Fluorescent Biosensor. *Biosens. Bioelectron.* **2020**, *165*, 112425. https://doi.org/10.1016/j.bios.2020.112425.

(29) Treon, S. P.; Chabner, B. A. Concepts in Use of High-Dose Methotrexate Therapy. *Clin. Chem.* **1996**, *42* (8), 1322–1329. https://doi.org/10.1093/clinchem/42.8.1322.